



HHS Public Access

Author manuscript

Nat Commun. Author manuscript; available in PMC 2014 May 02.

Published in final edited form as:

Nat Commun. 2013 ; 4: 2969. doi:10.1038/ncomms3969.

Binding of PHF1 Tudor to H3K36me3 enhances nucleosome accessibility

Catherine A. Musselman^{1,§}, Matthew D. Gibson², Erik W. Hartwick³, Justin A. North², Jovylyn Gatchalian¹, Michael G. Poirier², and Tatiana G. Kutateladze^{1,3}

¹Department of Pharmacology, University of Colorado School of Medicine, Aurora, Colorado 80045 USA.

²Department of Physics, Ohio State University, Columbus, Ohio 43210, USA.

³Program in Structural Biology and Biochemistry, University of Colorado School of Medicine, Aurora, Colorado 80045 USA.

Abstract

The Tudor domain of human PHF1 recognizes trimethylated lysine 36 of histone H3 (H3K36me3). This interaction modulates methyltransferase activity of the PRC2 complex and plays a role in retention of PHF1 at the DNA damage sites. We have previously determined the structural basis for the association of Tudor with a methylated histone peptide. Here we detail the molecular mechanism of binding of the Tudor domain to the H3K_C36me₃-nucleosome core particle (H3K_C36me₃-NCP). Using a combination of TROSY NMR and FRET we show that Tudor concomitantly interacts with H3K36me3 and DNA. Binding of the PHF1 Tudor domain to the H3K_C36me₃-NCP stabilizes the nucleosome in a conformation in which the nucleosomal DNA is more accessible to DNA-binding regulatory proteins. Our data provide a mechanistic explanation for the consequence of reading of the active mark H3K36me3 by the PHF1 Tudor domain.

INTRODUCTION

Human PHD finger protein 1 (PHF1) is found in major nuclear regulatory complexes. PHF1 is an accessory component of the Polycomb Repressive Complex 2 (PRC2) that methylates lysine 27 of histone H3 and is required for gene silencing (reviewed in¹). Upon genotoxic stress, PHF1 localizes to the sites of DNA damage through the association with DNA damage repair enzymes Ku70/Ku80². PHF1 contains an N-terminal Tudor domain that binds to trimethylated lysine 36 of histone H3 (H3K36me3)³⁻⁵. This interaction inhibits the

Users may view, print, copy, download and text and data- mine the content in such documents, for the purposes of academic research, subject always to the full Conditions of use: http://www.nature.com/authors/editorial_policies/license.html#terms

Correspondence should be addressed to: tatiana.kutateladze@ucdenver.edu.

[§]Present address: Department of Biochemistry, University of Iowa, Iowa City, Iowa 52242 USA.

Author contributions: C.A.M., M.G.P. and T.G.K. designed the study. C.A.M., M.D.G., E.W.H., J.A.N. and J.G. performed experiments and together with M.G.P. and T.G.K. analyzed the data. C.A.M. and T.G.K. wrote the manuscript with input from all authors.

Competing Financial Interest: The authors declare no competing financial interests.

methyltransferase activity of PRC2 and plays a role in the retention of PHF1 at the sites of double stranded DNA breaks³. We have previously determined the structural basis of Tudor association with a peptide corresponding to the H3K36me3 tail (residues 31-40 of H3)³. However, the question remains as to how the Tudor domain binds to H3K36me3 in the context of the full nucleosome and even further, the chromatin fiber. This is an especially pressing question given that the position of this histone mark would place Tudor just adjacent to the nucleosome core, which may greatly alter the interaction.

Although recent pioneering studies have begun shedding light on the mechanistic aspects for the association of effector domains with their target histone posttranslational modifications (PTMs) on the nucleosome⁶⁻¹⁰, there is still a dearth of such reports. This is in large part due to experimental limitations. Most of the detailed structural information regarding the nucleosome complexes has been obtained by X-ray crystallography. However, since the N-terminal histone tails protrude from the nucleosome core and are solvent accessible and flexible, it has proven difficult to study interactions of effectors with the modified tails using crystallographic methods. Currently only four nucleosome/effector complexes have been successfully crystallized, and all reveal interactions with the particle core (and unmodified H4 tail in the case of the Sir3 BAH domain)¹¹⁻¹⁷. As a result, various interactions with PTMs have been studied primarily using histone peptides, leaving a large gap in our knowledge of how these proteins bind to histone PTMs within the framework of the full NCP.

NMR spectroscopy is an ideal tool to address this question as it provides solution-state atomic resolution information and is very powerful in the detection and characterization of intermolecular interactions, even in very flexible constructs^{18,19}. However, it remains challenging to produce modified nucleosomes in amounts sufficient for NMR analysis. Moreover, due to the large size of the nucleosome/effector complexes, sophisticated labeling and advanced experimental methods are necessary to obtain quality data. Yet, progress is being made in this regard and exciting studies have recently demonstrated the influence of histone PTMs on the nucleosome and on the association with co-factors^{7,9}. The issues with the NCP size and amount can be overcome by studying the nucleosome/effector interactions using Förster Resonance Energy Transfer (FRET), which requires only nanomolar concentrations of the NCPs. FRET has previously been used to demonstrate that the entry/exit regions of nucleosomal DNA transiently unwrap from and rapidly rewrap onto the histone core surface²⁰⁻²². This phenomenon, which is often referred to as the DNA end 'breathing' motion, plays a fundamental role in nucleosome remodeling, DNA replication, and gene transcription.

Here we describe the mechanism for binding of PHF1 Tudor to the H3K_C36me3-NCP and characterize the effect of this interaction on targeting a specific DNA site within the NCP by a protein effector. We show that in addition to recognizing H3K36me3, the Tudor domain associates with DNA, and such multiple contacts may account for a higher affinity of Tudor for the H3K_C36me3-NCP. Interaction of the PHF1 Tudor domain with the H3K_C36me3-NCP facilitates *in vitro* binding of the DNA-specific protein LexA to the DNA site that is inaccessible in the fully wrapped nucleosome, thus suggesting a shift in equilibrium toward a more open form of the nucleosome. Together, our findings provide a possible mechanistic

explanation for the consequence of recognition of the H3K36me3 mark by the PHF1 Tudor domain.

RESULTS

Tudor binds to the H3K_C36me3 nucleosome

To determine the mechanism for recognition of the nucleosome by the Tudor domain of PHF1, we reconstituted the NCP carrying a methyl-lysine analogue (MLA) at position 36 of histone H3 (H3K_C36me3) (Supplementary Fig. S1). We generated the H3(C110A)K36C mutant and subjected it to alkylation by (2-bromoethyl) trimethylammonium bromide to yield the *N*-methylated aminoethylcysteine derivative. The MLA histone was refolded with unmodified recombinant H2A, H2B and H4, and the resulting histone octamer was assembled onto a Widom 601 DNA sequence through slow desalting. Because the size of the H3K_C36me3-NCP/Tudor complex (~205 kDa) is beyond the limit of conventional NMR, we generated the double ²D- and ¹⁵N-labeled Tudor domain and characterized its binding to H3K_C36me3-NCP using ¹H, ¹⁵N-transverse relaxation optimized spectroscopy (TROSY)-heteronuclear single quantum coherence (HSQC) experiments carried out at the elevated temperature of 310K, on a 900 MHz spectrometer equipped with a cryogenic probe.

The ¹H, ¹⁵N-TROSY-HSQC spectra were collected on the free protein and in the presence of increasing concentrations of H3K_C36me3-NCP and overlaid (Fig. 1a). Titration of the H3K_C36me3-NCP up to 0.1 mM induced significant changes in the Tudor amide resonances, which could be grouped into the three sets. One set of resonances showed a substantial decrease in intensity and disappeared completely upon addition of 0.05 mM of the nucleosome. The second set of crosspeaks gradually moved, revealing the fast-to-intermediate exchange regime on the NMR time scale. The third set was perturbed to a lesser degree. At a 1:1 molar ratio there was, on average, an ~80% decrease in resonance intensity, indicating a robust interaction between Tudor and the H3K_C36me3-NCP.

Plotting the intensity decrease ($1-I/I_0$) for each Tudor residue allowed us to identify the binding interface (Fig. 1b). Mapping the residues with rapidly disappearing amide signals onto the structure of the Tudor domain revealed an extensive patch at one of the open ends of the five-stranded β -barrel (Fig. 1c, magenta). Many of these residues are directly involved in the interaction with H3K_C36me3³. Particularly, the aromatic cage, where trimethylated Lys36 is bound (PHF1 residues W41, Y47, F65 and F71); the adjacent hydrophobic patch underneath Pro38 of the peptide (PHF1 residues L45 and L46); and the acidic groove (PHF1 residues E66, D67 and D68) were significantly perturbed upon addition of the H3K_C36me3-NCP. This binding interface matched well to the binding surface mapped based on chemical shift changes observed in the ¹⁵N-labeled Tudor domain as the H3K_C36me3 peptide was titrated in under similar conditions, i.e. 310K at 900 MHz (Fig. 1d, e). These results suggest that PHF1 Tudor binds to the methylated H3 tail of H3K_C36me3-NCP in a manner largely similar to how it associates with the histone peptide. However, several residues of PHF1 were perturbed by the nucleosome to a greater extent, specifically those that descend from the hydrophobic patch along the β 2 strand of the barrel, as well as from the acidic patch along the β 4 strand. In addition, R58 and E59 at the opposite end of the β -barrel were

affected only upon binding to the H3K_C36me₃-nucleosome, thus suggesting additional contacts with the intact NCP.

Recognition of the trimethylated Lys36 residue remains the major driving force for binding of the PHF1 Tudor domain to H3K_C36me₃-NCP. We tested the Y47A mutant of Tudor previously found to have impaired histone binding activity (Fig. 1f). Addition of H3K_C36me₃-NCP to the ¹⁵N-labelled Y47A mutant led to only a small and uniform decrease in resonance intensity, which is indicative of a very weak and non-specific association. These data reveal that a robust interaction with the NCP occurs only when Tudor is capable of binding to the H3K36me₃ mark.

Tudor has a high affinity for H3K_C36me₃-NCP

To assess the strength of the PHF1-NCP interaction, we carried out pulldown assays with GST-fusion Tudor domain (Fig. 2). GST-Tudor was incubated first with increasing concentrations of H3K_C36me₃-NCP and then with glutathione-agarose beads. After centrifugation, the nucleosome fraction bound to the protein was detected by western blot using an anti-H3 antibody (Fig. 2a). Densitometry analysis of the bound H3K_C36me₃-NCP yielded an apparent K_d of ~1.3 μ M (Fig. 2b), and revealed that binding of the PHF1 GST-fusion Tudor domain to H3K_C36me₃-NCP is stronger than its binding to the H3K36me₃ peptide alone (K_d = 36 μ M, ref.³). Pulldowns using Y47A mutant of GST-Tudor and the H3K_C36me₃-NCP, or wild type GST-Tudor and unmodified NCP showed much weaker associations. In agreement with NMR data, these results indicate that recognition of H3K36me₃ is the key requirement for PHF1 Tudor to bind the nucleosome, however additional contacts with the NCP beyond those with the histone tail contribute to the complex formation.

Tudor associates with DS-DNA

To explore whether the PHF1 Tudor domain makes contacts other than to the histone tail sequence in the nucleosome, we tested its ability to bind DNA. Titration of a 10 bp double-stranded (DS) DNA fragment into ¹⁵N-labelled Tudor induced substantial chemical shift changes in the protein (Fig. 3a, first panel). In contrast, titration of a single strand of the same DNA fragment did not lead to resonance perturbations, indicating that this interaction is specific for DS-DNA and likely depends on the presence of a major/minor groove (Fig. 3a, second panel). Analysis of the chemical shift perturbations (CSPs) afforded a K_d of 201 μ M for binding of the Tudor domain to the 10 bp DS-DNA. Furthermore, the 601 DNA sequence, which we used to reconstitute the H3K_C36me₃-NCP, caused large CSPs in the Tudor domain, which were generally similar in direction to those seen upon addition of the 10 bp DS-DNA, however the presence of ~14 major/minor grooves in the 601 DNA construct, and thus non-stoichiometric association, precluded a straightforward quantitative analysis of this interaction (Fig. 3a, third panel). Nevertheless, the pattern of CSPs inferred that the Tudor domain binds to DS-DNA in a non-specific manner. A plot of the resonance perturbations as a function of Tudor residue revealed that the residues involved in the interaction with DNA lay along the β -barrel sides and around the H3K36me₃ binding pocket (Fig. 3b, c). Subsequent titration of the H3K36me₃ peptide into the 10 bp DS-DNA-bound Tudor domain caused additional CSPs in the protein, and the intermediate exchange regime

indicated a stronger interaction with H3K36me3 (Fig. 3d). Together these data suggest that within the intact NCP the Tudor domain can concomitantly interact specifically with the methylated histone H3 tail as well as non-specifically with the nucleosomal DNA.

The model of the PHF1 Tudor/H3K_C36me₃-NCP complex

We generated a model of the PHF1 Tudor domain bound to the H3K_C36me₃-NCP using the docking program HADDOCK. A three body docking protocol utilizing Tudor/H3K36me₃ (4HCZ), the histone octamer with H3 cut at His39, and DNA (3LZ0) was applied. A total of ~64K restraints between the octamer and DNA were used, and Pro38 of the H3K36me₃ histone peptide was constrained to a bonding distance with His39 of the octamer either near the entry point of DNA or the exit point of DNA. Docking calculations of Tudor at either entry/exit point yielded very similar results, and comparison of the two models suggests that two Tudor domains can simultaneously associate with the NCP symmetrically trimethylated at Lys36 on both H3 tails (Fig. 4).

The model suggests that Tudor is stabilized at the H3K_C36me₃-NCP through concomitant interactions with the trimethylated histone tail and the minor groove and backbone of the nucleosomal DNA (Fig. 4). The Tudor domain is positioned between the two gyres of the DNA superhelix with the hydrophobic patch and β 1 and β 2 strands aligned with the minor groove of the DNA helical segment nearest the dyad. In addition, there are a few contacts between the residues in and around the Lys36me₃ binding pocket and the phosphate backbone of the entry/exit DNA. The model is in good agreement with CSPs observed upon titration of DS-DNA and the H3K_C36me₃-NCP, and although the full histone tail was not included in the docking algorithm, the orientation of the residues N-terminal to Lys36me₃ suggests that some of the additional CSPs seen upon titration of the H3K_C36me₃-NCP may be due to interactions between these histone residues and the Tudor domain in the context of the entire NCP.

We also note that during the docking calculation the DNA was extensively restrained on the octamer core. Our numerous attempts to examine the effect of the Tudor association on the NCP breathing dynamics by applying limited or no restraints at the entry/exit ends of DNA have failed. Nevertheless, modeling using the fully restrained NCP shows that the Tudor domain does not lock the DNA into a wrapped position at either orientation, implying that the entry/exit DNA can be readily lifted off the core.

Interaction with H3K36me₃ stabilizes a more open form of NCP

What is the consequence of binding of the PHF1 Tudor domain to H3K36me₃ in the NCP? The location of H3K36me₃ in the nucleosome readily positions this mark itself, as well as the PHF1 Tudor docking to this PTM, to influence nucleosomal DNA unwrapping/rewrapping or DNA accessibility and binding of regulatory proteins to DNA sites wrapped onto the nucleosome. We therefore investigated the impact of recognition of H3K36me₃ by the PHF1 Tudor domain on nucleosome unwrapping and binding of the DNA-specific repressor protein LexA using FRET (Fig. 5). H3K_C36me₃-NCPs were prepared with the 147 bp 601 nucleosome positioning sequence, this time with the LexA binding sequence replacing bases 8-27 (601L, Fig. 5a-c). The Cy3 donor fluorophore was attached to the 5

prime end of the 601L DNA molecule adjacent to the LexA site, and the Cy5 acceptor fluorophore was attached to H2A(K119C) (Fig. 5c). This positions Cy3 in the proximity of one of the Cy5 fluorophores so that there is significant energy transfer from fully wrapped nucleosomes (Fig. 5d), while a reduction in FRET efficiency implies a decrease in nucleosome wrapping^{21,23}.

We first examined the effect of H3K_C36me3 on nucleosome wrapping using LexA and Cy3-Cy5 labeled NCPs. The concentration of LexA required to bind 50% of the nucleosomes ($S_{1/2}$) is inversely proportional to the probability the LexA target site being unwrapped from the nucleosome for LexA binding²³ (Fig. 5b). Thus a reduction of $S_{1/2}$ induced by H3K_C36me3 would imply an increase in partial nucleosome unwrapping. Upon titration of LexA into Cy3-Cy5 labeled wild type NCP or H3K_C36me3-NCP we observed a decrease in FRET, due to LexA binding and stabilization of the unwrapped state. We found the LexA $S_{1/2}$ to be 3000 nM and 2400 nM for H3K_C36me3 and wild type nucleosomes, respectively (Fig. 5e). The similar $S_{1/2}$ values indicate that H3K_C36me3 itself does not directly impact nucleosome unwrapping.

We next titrated Tudor into 50 nM of wild type NCP or H3K_C36me3-NCP in the presence of 3 μ M ($S_{1/2}$) LexA. We found that above 30 μ M of PHF1 Tudor, the FRET efficiency is substantially reduced for nucleosomes containing H3K_C36me3, while the FRET efficiency for unmodified nucleosomes remains unchanged (Fig. 5f). This data indicate that Tudor binding to H3K_C36me3 disturbs the nucleosome, facilitating LexA binding to its target sequence buried within the nucleosome. This ability to facilitate LexA binding was further enhanced when a larger PHF1 construct, containing the Tudor domain and adjacent PHD1 finger, was examined (Fig. 6a). Because the PHD1 finger has no effect on binding of the Tudor domain to H3K36me3 (Fig. 6b) and shows no histone binding activity⁵, these results suggest that the increase in size of the NCP-interacting macromolecule produces the greater effect. Addition of PHF1 Tudor to the H3K_C36me3-nucleosomes in the absence of LexA resulted in no significant change in the FRET efficiency, implying that the presence of the DNA-binding target protein is essential for the enhancement of the DNA accessibility (Fig. 5g). Together, our findings support the previously proposed idea that transcription factor (TF) binding to a target site may expedite TF binding to a second target site further into the nucleosome^{24,25}, and provide the first example of such a heteromolecular augmentation (Fig. 6c).

DISCUSSION

In the past few years our knowledge of how reader domains bind PTMs on histone tails has grown significantly, however very few studies have investigated the mechanism of these associations in the context of the full nucleosome^{6-10,26}. We have previously determined the structural basis for the interaction of the PHF1 Tudor domain with a H3K36me3 peptide³. In this work, we characterize binding of PHF1 Tudor to the intact H3K_C36me3-NCP. We find that in addition to its histone binding capabilities, PHF1 Tudor interacts non-specifically with a double stranded DNA. The multiple interactions may account for the higher affinity of Tudor for the H3K_C36me3-NCP as compared to its affinity for the histone H3K36me3 peptide.

Dual association with H3K36me3 and nucleosomal DNA has recently been reported for the PWWP domain of LEDGF/PSIP1^{8,9}. Whereas PWWP binds to a DNA fragment or the H3K36me3 peptide with low affinities (K_d of ~150 μ M and 11-17 mM, respectively), bipartite binding to the H3K_C36me3-nucleosome results in a strong interaction (K_d of ~1.5 μ M)^{8,9}. Particularly, interaction with nucleosomal DNA was found to be responsible for a ~10⁴-fold enhancement in binding affinity and drives the recognition of the H3K_C36me3-NCP^{8,9}. Much like PWWP, the PHF1 Tudor domain binds to the H3K_C36me3-NCP with a ~1.3 μ M affinity, however its tight association with the H3K36me3 peptide alone (K_d of ~36 μ M) suggests that the recognition of methylated Lys36 is the driving force for the Tudor-H3K_C36me3-NCP interaction.

Nucleosomes have been shown to undergo spontaneous conformational fluctuations, in which a stretch of the entry/exit point DNA lifts off the histone core, providing transient access to the occluded regions of DNA for DNA-binding regulatory proteins and protein complexes^{20-22,27}. The unwrapping and following rewinding processes are fast, with spontaneous opening occurring within ~250 ms, and are widespread, with the DNA ends being unwrapped in 1-5% of NCPs at any point²⁰⁻²². On average, the NCP stays unwrapped only ~10-50 ms before rewinding²⁰. Within this short interval, some regulatory proteins are able to bind their respective target DNA sequences, but this time is not sufficient for RNA polymerase II (Pol II) to advance by even one base pair²⁰. It takes on average ~6-7 s for Pol II to elongate through the nucleosome, or ~2 s to process a ~40-50 bp linker DNA²⁰. Consequently, the NCP undergoes many cycles of rapid unwinding and rewinding before Pol II fully moves onto the nucleosome.

Our data demonstrate that interaction of the PHF1 Tudor domain with the H3K_C36me3-NCP facilitates binding of LexA to its target DNA sequence buried within the nucleosome, which is inaccessible in the fully wrapped NCP. This indicates a shift in equilibrium toward a more open form of the nucleosome and hindering the rewinding event in the presence of the DNA-binding protein. HADDOCK analysis of the Tudor-H3K_C36me3-NCP interaction suggests a mechanism for this shift. Because the Tudor domain binds H3K36me3 between the two gyres of the DNA superhelix and does not lock the DNA entry point, once the DNA lifts off, the bound PHF1 Tudor may sterically preclude rapid DNA rewinding, thus increasing the DNA accessibility to its ligand protein. Since the H3K36me3 mark is found in actively transcribed gene bodies, it will be interesting to explore the effect of the PHF1-H3K36me3 interaction on elongation activity of Pol II and whether this effect can be altered by chromatin fiber density and nucleosome positioning. Furthermore, it will be important to establish the significance of recognition of one H3K36me3 mark or two H3K36me3 marks on a single NCP. Lastly, future studies are also necessary to determine whether the nucleosomal changes imparted by Tudor association with H3K36me3 may play a role in PHF1 functions, particularly in modulating the methyltransferase activity of PRC2 and mediating PHF1 accumulation at DNA damage sites.

METHODS

DNA constructs and protein purification

The wild type PHF1 Tudor domain (residues 14-87 or residues 28-87) and Tudor-PHD1 (residues 14-140) were cloned from full length hPHF1 (obtained from Open Biosystems). Point mutant Y47A was generated by site-directed mutagenesis using the Stratagene QuickChange XL kit. Wild type and mutant proteins were expressed in *E. coli* BL21(DE3) pLysS cells grown in LB or $^{15}\text{NH}_4\text{Cl}$ supplemented M9-minimal media (grown in D_2O for purposes of NMR nucleosome binding studies) and induced with IPTG. Bacteria were harvested by centrifugation and lysed by sonication. The unlabeled, ^{15}N -labeled and $^2\text{D}/^{15}\text{N}$ -labeled GST-fusion proteins were purified using glutathione Agarose 4B beads (Fisher). The GST tag was either cleaved with PreScission protease, or left for the purposes of pulldowns, in which case the GST-fusion protein was eluted off the glutathione Agarose beads using 0.05 M reduced L-glutathione (Sigma Aldrich).

Xenopus histone proteins H2A, H2B, H3C110A, H3K36C/C110A, and H4 were expressed in *E. coli* BL21(DE3) pLysS cells grown in 2XYT media and induced with IPTG. Bacteria were harvested by centrifugation and lysed by sonication. Proteins were extracted from inclusion bodies, purified over ion exchange resin, and lyophilized. 32 repeats of the 601 Widom sequence were cloned into the pJ201 plasmid. The plasmid was purified in high yield primarily following the protocol outlined in²⁸. The individual sequences were released from the plasmid using EcoRV and purified away from the parental plasmid using PEG precipitation²⁹.

Methyl-lysine analogue generation

Histone H3(C110A)K36C point mutant was generated by site-directed mutagenesis using the Stratagene QuickChange XL kit and purified as described above. The histone H3K_C36me₃ was generated by alkylation of H3K36C with (2-bromoethyl) trimethylammonium bromide following the protocol outlined in³⁰. After desalting the protein was dialyzed into water and re-lyophilized.

HADDOCK modeling

HADDOCK modeling was performed via the webserver interface^{31,32}. The crystal structure Tudor in complex with the H3K36me₃ peptide (PDBID: 4HCZ) including peptide residues 31-38 was docked onto the 601-NCP crystal structure (PDBID: 3LZ0) with the H3 tail cut at His39. A three body docking protocol was followed, in which the histone octamer was taken as a single chain, the nucleosomal DNA as the second chain and the Tudor in complex with H3K36me₃ peptide as the third chain. Extensive unambiguous restraints were generated between the histone octamer and DNA and the peptide residue Pro38 and the histone octamer residue His39 were restrained to a bonding distance. Semi-flexibility options for the DNA and octamer were set to “none”, and the Tudor/peptide was set to automatic. The final model was chosen which had the best HADDOCK score and best fit for all restraints. In the final structure a covalent bonding distance was enforced between Pro38 and His39. Calculations were run for Tudor at both of the histone H3 tails in the NCP.

Nucleosome reconstitution

Equimolar ratios of H2A, H2B, H4 and either H3(C110A) or H3(C110A)_{K_C36me3} were mixed and refolded into 2 M NaCl, 10 mM Tris pH 7.5 and 5 mM β-mercaptoethanol (BME) to form the histone octamer²⁸. The octamer was purified by size exclusion chromatography on a sephacryl S-300 column. Purified octamer was mixed at a 1.2:1 ratio with purified 601 DNA and desalted according to protocol²⁸ into a final buffer of 20 mM Tris pH 7.5, 150 mM NaCl and 5 mM BME. The nucleosome was further purified from free DNA by sucrose gradient.

Pulldown assays

GST-fusion PHF1 Tudor was incubated with reconstituted H3K_C36me3- or wild type nucleosomes in binding buffer containing 20 mM Tris (pH 7.5), 150 mM NaCl, and 0.2 % Triton for 2 hours at 4C⁸. Glutathione-agarose beads were added and further incubated for 1 hour at 4C. Free nucleosome was washed away by washing 4X with 20 mM Tris (pH 7.5), 275 mM NaCl, and 0.2% Triton. Bound nucleosome was detected by western blot using an anti-H3 antibody (1:3000 dilution) (Abcam, AB1791). A control of nucleosome with beads alone (at the equivalent of a 0:10 molar ratio) was used to assess for non-specific binding. Blots were analyzed using ImageJ and normalized to account for non-specific binding. The apparent K_d was calculated using the equation:

$$Pixels = Pixels_{max} \left(([L] + [P] + K_d) - \sqrt{([L] + [P] + K_d)^2 - 4[P][L]} \right) / 2[P] \quad (1)$$

where [L] is concentration of the nucleosome, [P] is the concentration of Tudor, Pixels is the normalized pixel count calculated in ImageJ and Pixels_{max} is the count at saturation. For control, GST pulldown with H3K_C36me3-NCP was analyzed using Western blot, which was first probed with an anti-H3 antibody (Abcam ab1791) and then stripped with strip buffer (1.5% (w/v) glycine, 0.1% (w/v) SDS, 1% Tween-20, pH 2.2) for an hour, re-blocked, and probed with anti-GST-HRP antibody (GE Life Sciences RPN1236V) overnight.

NMR Spectroscopy

NMR experiments were collected on Varian 900 MHz and 600 MHz spectrometers equipped with a cryogenic probes at the University of Colorado School of Medicine NMR core facility. ¹H, ¹⁵N heteronuclear single quantum coherence (HSQC) or transverse relaxation optimized spectroscopy HSQC (TROSY-HSQC) experiments were carried out at 298K (peptide and 10 bp DNA) or 310K (nucleosome and 601 DNA) on ¹⁵N- or ²D/¹⁵N-labeled Tudor (wild type or mutant) or Tudor-PHD1 in 20 mM Tris pH 6.8 and 150 mM NaCl. Spectra were recorded in the presence of increasing concentrations of H3K36me3 peptide (synthesized by the University of Colorado Peptide Core Facility), 10 bp SS-DNA, 10 bp DS-DNA, 601 DNA or reconstituted nucleosomes. K_d value for the Tudor-DS-DNA interaction was calculated by a nonlinear least-squares analysis in Kaleidagraph using the equation:

$$\Delta\delta = \Delta\delta_{max} \left(([L] + [P] + K_d) - \sqrt{([L] + [P] + K_d)^2 - 4[P][L]} \right) / 2[P] \quad (2)$$

where [L] is concentration of DS-DNA, [P] is concentration of the protein, δ is the observed normalized chemical shift change and δ_{\max} is the normalized chemical shift change at saturation, calculated as

$$\Delta\delta = \sqrt{(\Delta\delta H)^2 + (\Delta\delta N/5)^2} \quad (3)$$

where δ is the chemical shift in parts per million (ppm).

Nucleosome and LexA Preparation for FRET Measurements

Nucleosomal DNA, 601L was prepared by PCR from a plasmid containing the LexA binding site at bases 8-27 with the Cy3-labeled oligonucleotide, Cy3-CTGGAGATACTGTATGAGCATACAGTACAATTGGTC and the unlabeled oligonucleotide, ACAGGATGTATATATCTGACACGTCGCTGGAGACTA. The Cy3 labeled oligonucleotide was labeled using a Cy3-NHS ester (GE Healthcare) at a 5' amino group and purified by RP-HPLC on a 218TPTM C18 (Grace/Vydac) column. *Xenopus* histones were expressed and purified as in²⁸. All H3 histones contained the H3C110A mutation. LexA was expressed and purified by known methods.

H3K_C36me₃ was prepared as reported^{30,33}. Briefly, recombinant H2AK119C and H2B were refolded into heterodimer and then labeled with Cy5-maleamide (GE Healthcare).

Heterodimer was first reduced in 10 mM TCEP pH 7.1 for 0.5 hours, and then dialyzed against 5 mM sodium PIPES pH 6.1, 2 M NaCl. After reclaiming, heterodimer was purged under argon at 4°C for 30 minutes, and 2M HEPES pH 7.1 was bubbled with argon at 4°C for 5 minutes. The Cy5-maleamide was dissolved in anhydrous DMF to a concentration of 22 mM and added to heterodimer in a 25-fold molar excess. Sample was gently rotated for 1 hour at room temperature and overnight at 4°C. The heterodimer was then purified by gel filtration on a Superdex 200 column. The labeling efficiency for the reaction was 88% as measured by UV-Vis absorption. H3K_C36me₃ and unmodified H3 were separately refolded with H4 into tetramer. H3-H4 tetramer in 0.5 mM potassium phosphate (pH 7.5) with 2 M NaCl was then combined with 10% excess Cy5 labeled H2AK119C-H2B heterodimer in 5 mM pipes (pH 6.1) with 2 M NaCl and incubated at 4°C overnight to form histone octamer. The resulting octamer was purified by gel filtration on a Superdex 200 column.

Nucleosomes were reconstituted by double dialysis with 10% excess 601L DNA into 0.5 mM potassium phosphate (pH 7.5) with 1 mM BZA. Reconstituted nucleosomes were purified by 5-30% sucrose gradient.

FRET measurements

All FRET efficiency measurements were determined from spectra acquired by a Horiba Scientific Fluoromax 4. Samples were excited at 510 and 610 nm and the photoluminescence spectra were measured from 530 to 750 nm and 630 to 750 nm for donor and acceptor excitations, respectively. Each wavelength was integrated for one second, and the excitation and emission slit width were set to 5 nm with 2 nm emission wavelength steps. FRET measurements were computed through the (ratio)_A method.

LexA titrations were carried out in 75 mM NaCl, 0.1 mM potassium phosphate pH 7.5, 11.5 mM Tris-HCL pH 7.5, 0.00625% IGEPAL, and 0.00625% TWEEN20 with 10 nM nucleosomes. PHF1 Tudor and Tudor-PHD1 titrations were carried out with or without 3 μ M LexA in 75 mM NaCl, 62.5 μ M potassium phosphate pH 7.5, 15.25 mM Tris pH 7.5, 0.00625% IGEPAL, 0.00625% TWEEN20 with 50 nM nucleosomes. The nucleosome concentration was increased to 50 nM to compensate for increased background caused by the addition of PHF1. The change in nucleosome concentration does not impact the FRET measurements because the $(\text{ratio})_A$ method is insensitive to fluorescence intensity, and does not impact LexA and PHF1 Tudor binding as both concentrations are significantly below the micromolar concentrations required for LexA and PHF1 Tudor binding. FRET values in each titration were normalized to the FRET efficiency in the absence of the titrant. Titrations were fit to $E = (E_f - E_0)/(1 + (S_{1/2}/C) + E_0$, where E is the FRET efficiency at concentration C of the titrant, E_0 the efficiency in the absence of the titrant, E_f the efficiency at high titrant concentration, and $S_{1/2}$ is the inflection point. Errors in Figures 5 and 6 represent a standard deviation based on three experiments (PHF1 titrations) or two experiments (LexA titrations). Errors for fits represent 68% confidence bounds.

Supplementary Material

Refer to Web version on PubMed Central for supplementary material.

ACKNOWLEDGMENTS

We thank Morgan Welsh Bernier and Andrew Slater for help with nucleosome sample preparation. This research is supported by grants from the NIH, GM096863 and GM101664 (to T.G.K.), and GM083055 (to M.G.P.), and by Career Award in Basic Biomedical Sciences from the Burroughs Wellcome Fund (to M.G.P.). C.A.M. is supported by Cancer League of Colorado.

REFERENCES

1. Margueron R, Reinberg D. The Polycomb complex PRC2 and its mark in life. *Nature*. 2011; 469:343–349. [PubMed: 21248841]
2. Hong Z, et al. A polycomb group protein, PHF1, is involved in the response to DNA double-strand breaks in human cell. *Nucleic Acids Res*. 2008; 36:2939–2947. [PubMed: 18385154]
3. Musselman CA, et al. Molecular basis for H3K36me3 recognition by the Tudor domain of PHF1. *Nat Struct Mol Biol*. 2012; 19:1266–1272. [PubMed: 23142980]
4. Cai L, et al. An H3K36 methylation-engaging Tudor motif of polycomb-like proteins mediates PRC2 complex targeting. *Mol Cell*. 2013; 49:571–582. [PubMed: 23273982]
5. Qin S, et al. Tudor domains of the PRC2 components PHF1 and PHF19 selectively bind to histone H3K36me3. *Biochem Biophys Res Commun*. 2013; 430:547–553. [PubMed: 23228662]
6. Canzio D, et al. Chromodomain-mediated oligomerization of HP1 suggests a nucleosome-bridging mechanism for heterochromatin assembly. *Mol Cell*. 2011; 41:67–81. [PubMed: 21211724]
7. Munari F, et al. Methylation of lysine 9 in histone H3 directs alternative modes of highly dynamic interaction of heterochromatin protein hHP1beta with the nucleosome. *J Biol Chem*. 2012; 287:33756–33765. [PubMed: 22815475]
8. Eidahl JO, et al. Structural basis for high-affinity binding of LEDGF PWWP to mononucleosomes. *Nucleic Acids Res*. 2013; 41:3924–3936. [PubMed: 23396443]
9. van Nuland R, et al. Nucleosomal DNA binding drives the recognition of H3K36- methylated nucleosomes by the PSIP1-PWWP domain. *Epigenetics & chromatin*. 2013; 6:12. [PubMed: 23656834]

10. Lu X, et al. The effect of H3K79 dimethylation and H4K20 trimethylation on nucleosome and chromatin structure. *Nat Struct Mol Biol.* 2008; 15:1122–1124. [PubMed: 18794842]
11. Barbera AJ, et al. The nucleosomal surface as a docking station for Kaposi's sarcoma herpesvirus LANA. *Science.* 2006; 311:856–861. [PubMed: 16469929]
12. Makde RD, England JR, Yennawar HP, Tan S. Structure of RCC1 chromatin factor bound to the nucleosome core particle. *Nature.* 2010; 467:562–566. [PubMed: 20739938]
13. Armache KJ, Garlick JD, Canzio D, Narlikar GJ, Kingston RE. Structural basis of silencing: Sir3 BAH domain in complex with a nucleosome at 3.0 Å resolution. *Science.* 2011; 334:977–982. [PubMed: 22096199]
14. Kato H, et al. A conserved mechanism for centromeric nucleosome recognition by centromere protein CENP-C. *Science.* 2013; 340:1110–1113. [PubMed: 23723239]
15. Arnaudo N, et al. The N-terminal acetylation of Sir3 stabilizes its binding to the nucleosome core particle. *Nat Struct Mol Biol.* 2013; 20:1119–1121. [PubMed: 23934150]
16. Yang D, et al. Nalpha-acetylated Sir3 stabilizes the conformation of a nucleosome-binding loop in the BAH domain. *Nat Struct Mol Biol.* 2013; 20:1116–1118. [PubMed: 23934152]
17. Wang F, et al. Heterochromatin protein Sir3 induces contacts between the amino terminus of histone H4 and nucleosomal DNA. *Proc Natl Acad Sci U S A.* 2013; 110:8495–8500. [PubMed: 23650358]
18. Kato H, et al. Architecture of the high mobility group nucleosomal protein 2- nucleosome complex as revealed by methyl-based NMR. *Proc Natl Acad Sci U S A.* 2011; 108:12283–12288. [PubMed: 21730181]
19. Zhou BR, et al. Histone H4 K16Q mutation, an acetylation mimic, causes structural disorder of its N-terminal basic patch in the nucleosome. *J Mol Biol.* 2012; 421:30–37. [PubMed: 22575889]
20. Li G, Levitus M, Bustamante C, Widom J. Rapid spontaneous accessibility of nucleosomal DNA. *Nat Struct Mol Biol.* 2005; 12:46–53. [PubMed: 15580276]
21. Li G, Widom J. Nucleosomes facilitate their own invasion. *Nat Struct Mol Biol.* 2004; 11:763–769. [PubMed: 15258568]
22. Poirier MG, Bussiek M, Langowski J, Widom J. Spontaneous access to DNA target sites in folded chromatin fibers. *J Mol Biol.* 2008; 379:772–786. [PubMed: 18485363]
23. North JA, et al. ATP-dependent nucleosome unwrapping catalyzed by human RAD51. *Nucleic Acids Res.* 2013
24. Adams CC, Workman JL. Binding of disparate transcriptional activators to nucleosomal DNA is inherently cooperative. *Mol Cell Biol.* 1995; 15:1405–1421. [PubMed: 7862134]
25. Polach KJ, Widom J. A model for the cooperative binding of eukaryotic regulatory proteins to nucleosomal target sites. *J Mol Biol.* 1996; 258:800–812. [PubMed: 8637011]
26. Musselman CA, Lalonde ME, Cote J, Kutateladze TG. Perceiving the epigenetic landscape through histone readers. *Nat Struct Mol Biol.* 2012; 19:1218–1227. [PubMed: 23211769]
27. Koopmans WJ, Buning R, Schmidt T, van Noort J. spFRET using alternating excitation and FCS reveals progressive DNA unwrapping in nucleosomes. *Biophysical journal.* 2009; 97:195–204. [PubMed: 19580757]
28. Luger K, Rechsteiner TJ, Richmond TJ. Expression and purification of recombinant histones and nucleosome reconstitution. *Methods in molecular biology.* 1999; 119:1–16. [PubMed: 10804500]
29. Lis JT, Schleif R. Size fractionation of double-stranded DNA by precipitation with polyethylene glycol. *Nucleic Acids Res.* 1975; 2:383–389. [PubMed: 236548]
30. Simon MD, et al. The site-specific installation of methyl-lysine analogs into recombinant histones. *Cell.* 2007; 128:1003–1012. [PubMed: 17350582]
31. Dominguez C, Boelens R, Bonvin AM. HADDOCK: a protein-protein docking approach based on biochemical or biophysical information. *Journal of the American Chemical Society.* 2003; 125:1731–1737. [PubMed: 12580598]
32. de Vries SJ, van Dijk M, Bonvin AM. The HADDOCK web server for data- driven biomolecular docking. *Nature protocols.* 2010; 5:883–897. [PubMed: 20431534]

33. Shimko JC, North JA, Bruns AN, Poirier MG, Ottesen JJ. Preparation of fully synthetic histone H3 reveals that acetyl-lysine 56 facilitates protein binding within nucleosomes. *J Mol Biol.* 2011; 408:187–204. [PubMed: 21310161]

Author Manuscript

Author Manuscript

Author Manuscript

Author Manuscript

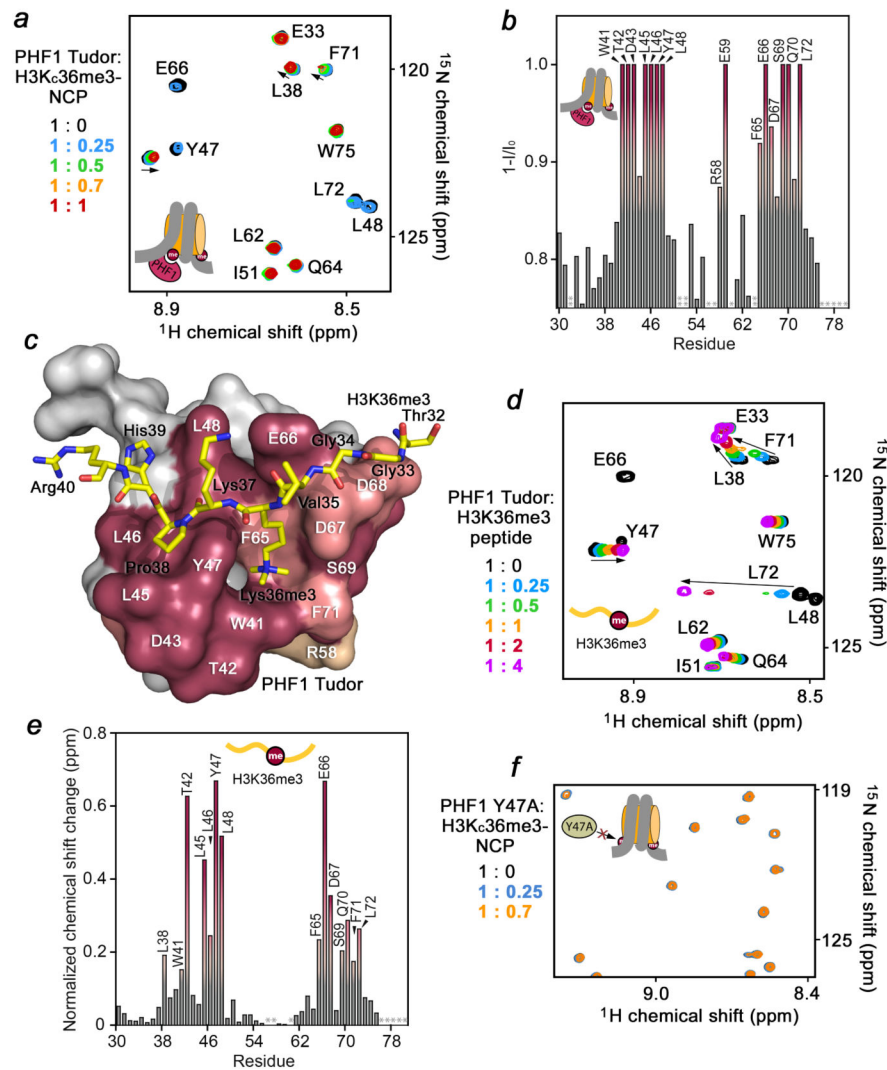


Figure 1. Tudor interacts with the H3K_C36me₃-nucleosome

(a) ^1H , ^{15}N TROSY-HSQC spectral overlays of wild type Tudor in the presence of increasing concentrations of H3K_C36me₃-NCP (molar ratio is shown to the left). (b) A plot of the decrease in resonance intensity ($1-I/I_0$) induced by the H3K_C36me₃-NCP as a function of Tudor residue. Decreases of greater than 85%, 90% and 96% are shown in tan, salmon and mauve respectively. An asterisk indicates a missing or unassigned peak. The double asterisk indicates value below shown threshold. (c) Residues demonstrating significant decreases in resonance intensity are mapped onto a surface representation of Tudor with the H3K36me₃ peptide shown as sticks in yellow. Residues of the H3K36me₃ peptide and the Tudor domain are labeled using a three-letter code and a one-letter code, respectively. (d) ^1H , ^{15}N HSQC spectral overlays of wild type Tudor in the presence of increasing concentrations of H3K36me₃ peptide. (e) A plot of the extent of normalized chemical shift change induced by the H3K36me₃ peptide as a function of Tudor residue, with changes greater than the average, average plus 1/2 or average plus 1 standard deviation shown in tan, salmon and mauve respectively. An asterisk indicates a missing or unassigned

peak. (f) ^1H , ^{15}N TROSY-HSQC spectral overlay of Y47A Tudor mutant in the presence of increasing concentrations of the H3K_C36me₃-NCP (molar ratio shown to the left).

Author Manuscript

Author Manuscript

Author Manuscript

Author Manuscript

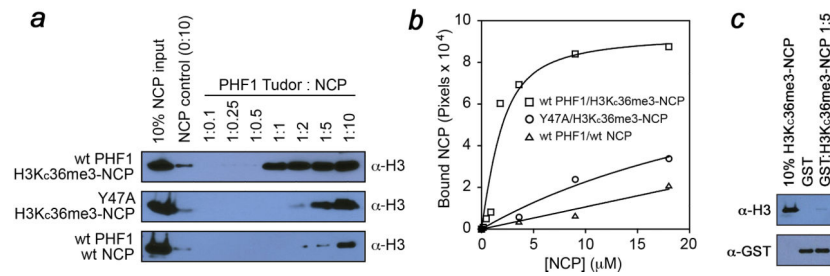


Figure 2. Tudor interaction with the nucleosome is dependent on methylation at H3K36

(a) Western analysis of pull-downs of wild type GST-Tudor with H3K_C36me₃-NCP (top) of Y47A GST-Tudor with H3K_C36me₃-NCP (middle) or wild type GST-Tudor with the unmodified wild type NCP (bottom). (b) The representative binding curves shown for each combination of the Tudor domain and NCP. Densitometry analysis of the bound H3K_C36me₃-NCP reveals an apparent affinity of 1.3 ± 0.5 μM (S.D. based on three experiments) of wild type GST-Tudor (squares), and significantly weaker association of the Y47A mutant GST-Tudor with H3K_C36me₃-NCP (circles) or wild type Tudor with wild type nucleosomes (triangles). All experiments were performed in triplicate. (c) Western blot analysis of GST pull-down with H3K_C36me₃-NCP showing that GST does not bind to H3K_C36me₃-NCP.

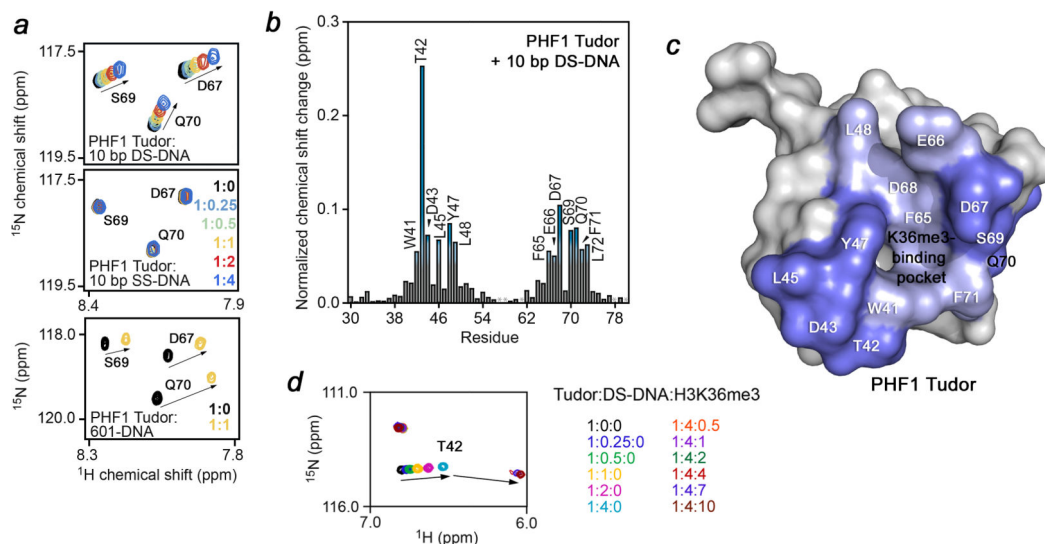


Figure 3. Tudor interacts non-specifically with double stranded DNA

(a) ^1H , ^{15}N HSQC overlay of Tudor in the presence of increasing concentrations of a 10 bp fragment of double stranded (top) or single stranded (middle) DNA or the double stranded Widom 601 DNA sequence (bottom). (b) A plot of the normalized chemical shift change induced upon titration of the 10 bp DS-DNA fragment as a function of Tudor residue, with changes greater than the average plus 1/3 and average plus 2/3 the standard deviation shown in light blue and dark blue, respectively. (c). Residues showing significant chemical shift changes in (b) are mapped onto a surface representation of Tudor. (d) The Tudor domain binds weaker to DS-DNA and stronger to H3K36me3. Superimposed ^1H , ^{15}N HSQC spectra of the Tudor domain collected upon addition of a 10 bp DS-DNA fragment (fast exchange regime), followed by addition of H3K36me3 peptide (intermediate exchange regime). Molar ratios of Tudor to DNA to peptide are shown to the right.

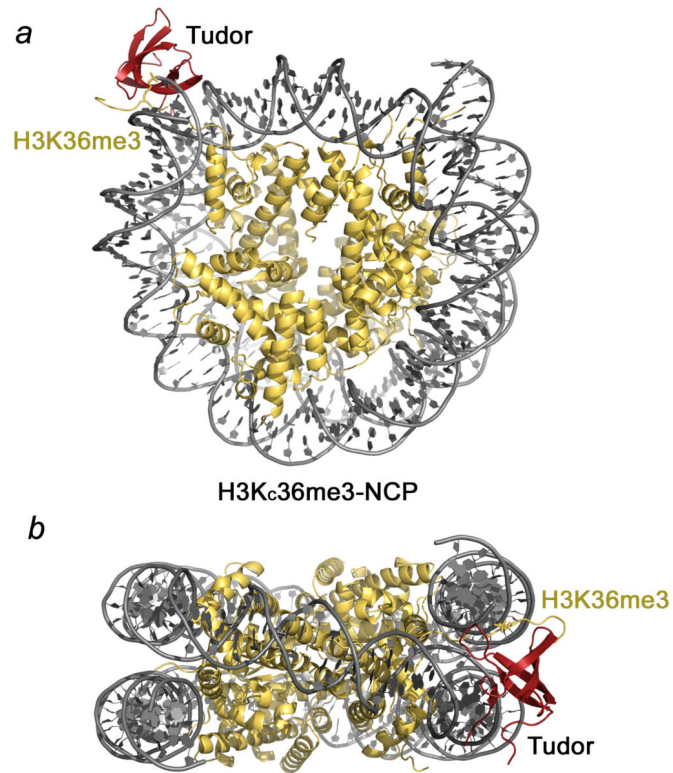


Figure 4. A model of the Tudor/H3K_C36me₃-NCP complex
HADDOCK model of Tudor bound to the H3K_C36me₃-NCP. The Tudor domain is shown in mauve, nucleosomal DNA in gray and histones in yellow. The Lys36me₃ residue is shown as sticks. Docking calculations were performed for Tudor at both histone H3 tails near the entry (a) and exit (b) regions of the DNA.

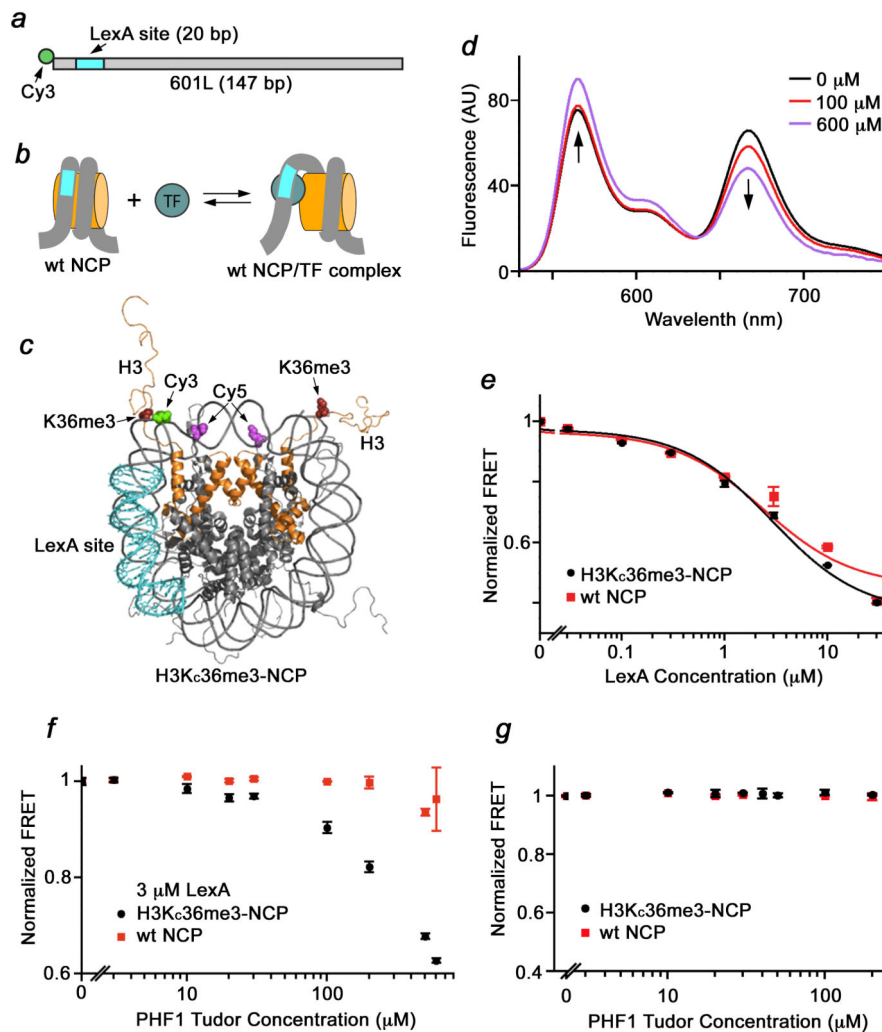


Figure 5. PHF1 Tudor binding to the H3K_C36me₃-NCP stabilizes a more open form of the nucleosome
 FRET measurements of the influence of PHF1 Tudor on TF binding. (a) Diagram of the 601L DNA molecule. (b) A two-state model of TF binding to its target site within the nucleosome. (c) Crystal structure of the NCP (PDB ID: 1KX5) that indicates the positions of H3 (orange); MLA at H3K36C (dark red); Cy5 at H2AK119C (purple); Cy3 at the 5 prime end of 601L (green); and the LexA target site (cyan). (d) Fluorescence spectra with Cy3-Cy5 labeled H3K_C36me₃-NCPs with 3 μM of LexA and either 0 μM (black), 10 μM (red) and 600 μM (purple) of PHF1 Tudor. The Cy3 emission increases as the Cy5 emission decreases indicating a decrease in FRET efficiency. (e) FRET efficiencies of LexA titrations with H3K_C36me₃ (black) and unmodified wt nucleosomes (red). FRET efficiencies were done in duplicate and fit to a noncooperative binding curve with $S_{1/2}$ of 3000 ± 600 nM and 2400 ± 900 nM for H3K_C36me₃ and unmodified wt nucleosomes, respectively. (f, g) FRET efficiencies of PHF1 Tudor titrations with (f) and without (g) 3 μM LexA and either H3K_C36me₃ (black) or unmodified NCPs (red). Error bars represent a standard deviation based on three experiments (PHF1 titrations) or two experiments (LexA titrations).

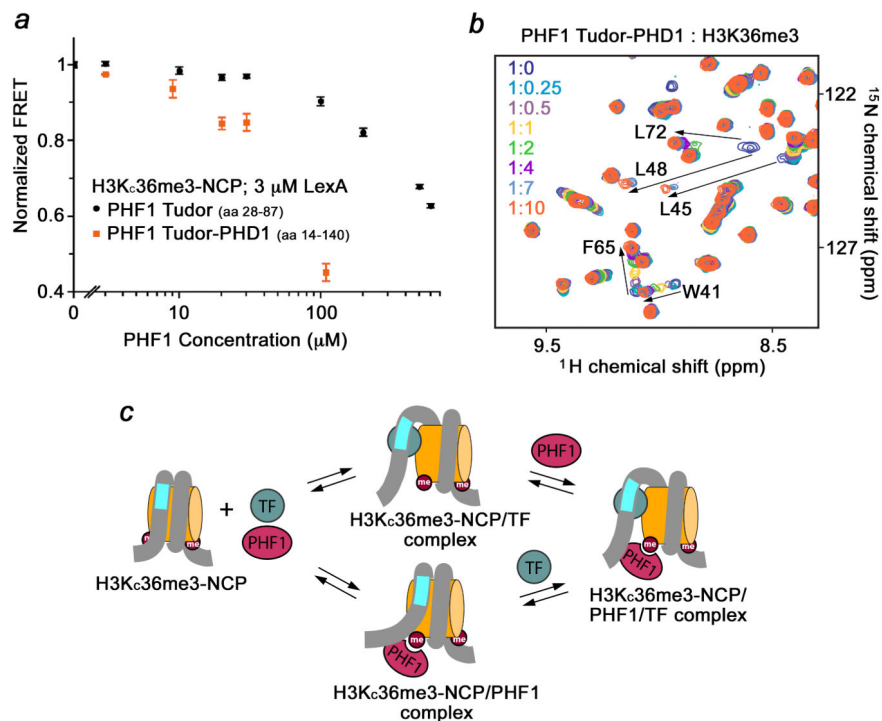


Figure 6. The larger PHF1 construct containing Tudor and PHD1 further enhances LexA binding

(a) FRET efficiencies of the PHF1 Tudor (black) and Tudor-PHD1 (orange) titrations with H3K_c36me₃ nucleosomes in the presence of 3 μM LexA. Error bars represent a standard deviation based on three experiments. (b) Superimposed ^1H , ^{15}N HSQC spectra of PHF1 Tudor-PHD1 recorded as H3K_c36me₃ peptide was titrated in. An almost identical pattern of chemical shift changes was observed in the Tudor domain linked to the PHD1 finger, as compared to the changes seen in this domain alone (see ref.³). Arrows indicate most notable changes. Resonances corresponding to the PHD1 finger were unperturbed, implying that PHD1 is not involved in this interaction. (c) Four-state model of PHF1 Tudor and LexA binding to nucleosomes.